Numerical Methods in Civil Engineering

Journal Homepage: https://nmce.kntu.ac.ir/

Proposal of the Location and Shape of the Outrigger Arm and Belt Truss in the High-Rise Buildings with the Central Core

Gholamreza Abdollahzadeh*, Hadi Faghihmaleki and Reza Alghosi *****

ARTICLE INFO

RESEARCH PAPER

Article history:
Received:
September 2021.
Revised:
March 2022.
Accepted:
April 2022.

Keywords:
Soft computing,
Soil infiltration,
GEP,
Coefficient of permeability,
Statistical parameters

Abstract:

The outrigger arm system and belt truss with braced core in the center of the structure surrounded by belts truss, is an efficient and reliable system for high-rise buildings against severe lateral forces such as earthquake and wind. The purpose of this research is investigating the outrigger arm system and belt truss with the braced core under lateral loads. Another purpose of this research is to reduce the drift and displacement of the roof against these loads with deformation and finding the optimal location for the outrigger arm through various methods. Analysis of nonlinear time history and spectral analysis of the site with a high relative risk for the three models of 30, 45, and 60 floors have shown that the optimum location of the outrigger arm and belt truss with the proposed method in this research has been better more noteworthy than the previous methods and caused decreasing as it has induced about a decrease in absolute roof displacement and maximum relative displacement of floors. The suggested deformation for outrigger arm in addition to reducing the stress concentration in the floors where outrigger arm are is installed, has caused a significant reduction in the absolute change in the roof of the building and the maximum relative displacement of the floors.

1. Introduction

Construction of high-rise buildings first began with the goal of defense, followed by the symbolic and applied aspects. The growth and development of new high-rise buildings began in the 19th century with commercial and household use [1]. The growing use of high-resistance materials and advanced construction techniques is combined with the needs of urbanization, which has led to a significant increase in the number and variety of tall structures. The extra-long building with the mega frame system has had a huge effect on the economy and society [2-4]. One can say that a long structure follows two goals: Technical rules and aesthetic issues.

The first objective, technical performance, is to achieve structure stability and resistance against forces applied to the structure.

Buildings are exposed to various loads such as wind and snow loads, the weight of components, residents and equipment, and also earthquakes and extreme earth movements in many parts of the world, and therefore ought to resist them. The structure remains stable by resisting loads and transmitting them to the ground through building components. In order to ensure that the building can withstand such loads without deformation or severe collapse, prior scientific analysis and theory must be performed. The second objective is the aesthetic function, which is mainly applied within the scope of architectural engineering and as an intuitive tool. Both the technical and aesthetic conditions of a long structure must be met at the same time, so that the structure, in addition to technical issues, justifies other matters. After considering all aspects of creating a high-rise structure, a suitable structure system should be embedded for the building. One of the most important issues facing the designers is to choose the type of system resistance to withstand the loads applied to the buildings. It should be noted that designers can determine the best type of structural system and construct the design based on it.

* *Professor, Faculty of Civil Engineering, Babol Noshirvani University of Technology, Iran.*

** *Corresponding author: Assistant Professor, Faculty of Civil Engineering, Ayandegan Institute of Higher Education, Tonekabon, Iran. Email: h.faghihmaleki@gmail.com*

*** *M.Sc. Student, Faculty of Civil Engineering, Tabari University of Babol, Iran.*

One of the economic means approved for the construction of high buildings is the use of a frame with outrigger arm and belt truss [5].

Modern and flexible buildings have sophisticated structural systems which include various components, with complex features and large [6- 8]. With increasing height, seismic design is challenging in terms of stiffness, strength and stability, especially in high seismicity. Compared to medium and low height buildings, the restrained frame systems in high-rise buildings offer a distinct feature in their behavior and special aspects in design, including long period and effects of higher modes [9 and 10].

The outrigger arm system is the modified form of bracing frames and the frame with a shear wall, and is used in steel, concrete and composite structures. A tall, arm restrained structure consists of a central reinforced concrete core or restrained steel frame which is attached to the outer pillars by a horizontal beam. The core may be located in the middle of the building plan, and the outrigger arm is placed on either side of the building, or it may be located on one side of the building, and horizontal beams are connected to the columns on the other side. When the building is under the influence of a horizontal load, the outrigger arm prevents the core from rotating, and causes the core lateral displacements and moments to be less than the outrigger arm-free case. As a result, the depth of the impact of the structure increases during console by tension in the wind side columns and compression in the opposite side columns. In addition to the end columns of the outrigger arms, other peripheral pillars are also usually used to support the outrigger arms. This is done by adding a deep beam or belt around the structure and at the level of the outrigger arm. This type of structural form is called a structure with belt truss [1].

For the analysis of peripheral frames, several methods for controlling the building with this system are presented against lateral loads. In 1975, Coull and Bose [11] proposed a method based on the theory of elasticity. In this method, the structure is modeled as orthotropic equivalent plates, and equilibrium and consistency equations are satisfied in the equivalent structure. In 1978, Coull and Ahmed [12] presented a method for obtaining the displacement of the peripheral frame. Connor and Pouangare in 1991 [13], proposed the method of five vertical members, in which the structure equates to vertical beams and planes, and by calculating the shear and bending stiffness of the members, relations are obtained for the stresses in the columns. Jahanshahi et al. in 2012 [13], in their article provided an effective method for static analysis of high-rise buildings with the combined system of the peripheral frame and outrigger arm system and belt truss, taking into account the shear moment effects. Abdi-Moghaddam et al. in 2015 [14], have reviewed the Outrigger arm system and the belt truss under a near-area earthquake. In the year 2016, Brunesi et al. [15], reviewed two models of 30 and 60 floors with an Outrigger arm system and the belt truss under the near and far-area and near earthquake, and compared these systems by spectral analysis, eventually concluding that this system is sensitive to height and designing must be conform to high accuracy along with increasing the height. Kim and Park in 2012 [16], evaluated the progressive collapse potential of building structures with core and outrigger trusses using nonlinear static and dynamic analyses. According to dynamic analysis results, they concluded that the vertical displacement monotonically increased until collapse as a result of buckling of some of outrigger truss members. However the structure with outrigger and belt trusses remained stable after a perimeter column was removed. Chen and Zhang in 2017 and Hoenderkamp in 2008 [17 and 18], investigated the optimum location and number of outriggers in high rise buildings and the seismic performance of outrigger braced structures were investigated by other researches. In the year 2017, Kim and Kang in 2017 [19], examined a damper in the outrigger system. Numerical analysis showed that the smart outrigger damper system could provide superior control performance for the reduction of both wind and earthquake responses compared to the general outrigger system and passive outrigger damper system. Kamgar and Rahgozar in 2017 [20], investigated the optimum location of outriggers in high rise buildings, based on maximizing the outrigger-belt truss system's strain energy, and presented a methodology for determining the optimum location of a flexible outrigger system ~~is~~. Accuracy of the proposed method is verified through numerical examples. The results show that the proposed method is reasonably accurate. In addition, for different stiffness of shear core and outrigger system, several figures are presented that can be used to determine the optimum location of belt truss and outrigger system.

2. Non-linear dynamic structural analysis

In order to use the steel's ductility, force must be increased so that its section can flow, then the steel will have the ability to deform keeping resistance (entering the nonlinear range). When steel can deform while keeping its strength, it can in fact resist a force greater than the force that enters it, as it can absorb and dampen a larger force by its own deformation. Simply put, when the lateral force enters the structure, the structure has a linear behavior before the sections flow, that is, the relationship between the base shear and the displacement of the roof is linear, and by removing the lateral force, the structure will be in its previous state without permanent deformation (plastic deformation). In the meantime, in this step, as the lateral force increases, the force of the elements also increases and the sections of the elements become larger in design (Standard 2800, 2019) [21].

Dynamic analysis of nonlinear time histories is a powerful and effective tool for determining seismic demands, also used to identify the plastic joint mechanism in a building. Conversely, in the underlying analysis, there are several inherent deficiencies and limitations [22] for example, constant load distribution, uncertainty in calculations in the effects of higher modes, in the modal method, uncertainty in the composition of different modal contingencies, and underestimating plastic rotation in joint [22]. Consequently, with the rapid development of computer technology and computational algorithms for nonlinear dynamic analysis, it has now become a suitable method for examining and designing of high-rise buildings. Therefore, due to the capabilities of this analytical method, in this research, the nonlinear dynamic analysis has been used to assess the behavior of tall buildings of 30, 45 and 60 floors, as well.

2.1 Structural Modeling and Design

Figure 1 schematically shows three models of 30, 45 and 60 floors, and a sample way of placing the outrigger arm. Buildings have been constructed in an area with soil shear wave velocity of 180 m/s <VS<360 m/s and according to the ASCE 7-10 regulation, is a type D soil (ASCE, 2010) [12]. Figure 2 shows how the outrigger arm and belt truss are placed. The central core is a 16x16 m square in the plan, fitted with a CBF brace and connected to the box columns by the outrigger arm. The three structural designs studied in this research are symmetrical in plan with squares of 48×48 m in each floor, the distance of their columns from each other (S) is 8 meters in both directions longitudinally and transversely and the height of the columns (H) is 4 meters. The total heights of buildings are 120, 180 and 240 meters respectively for H-01, H-02 and H-03 models. For all three models, according to ASCE 7-10 American Loading Regulation (ASCE, 2010) [12], the dead and live floor loads were respectively, 453 kg/m2 and 350 kg/m2, and for the roof , dead and live, and snow loads were considered 412 kg/m2, 150 kg/m2, and 150 kg/m2, respectively. For columns, beams and braces, the steel with ultimate strengths of 450 N/m2, 275 N/m2, and 700 N/m2 (ANSI/AISC, 2010) are used, respectively. General geometry and loading of different models are summarized in Table 1

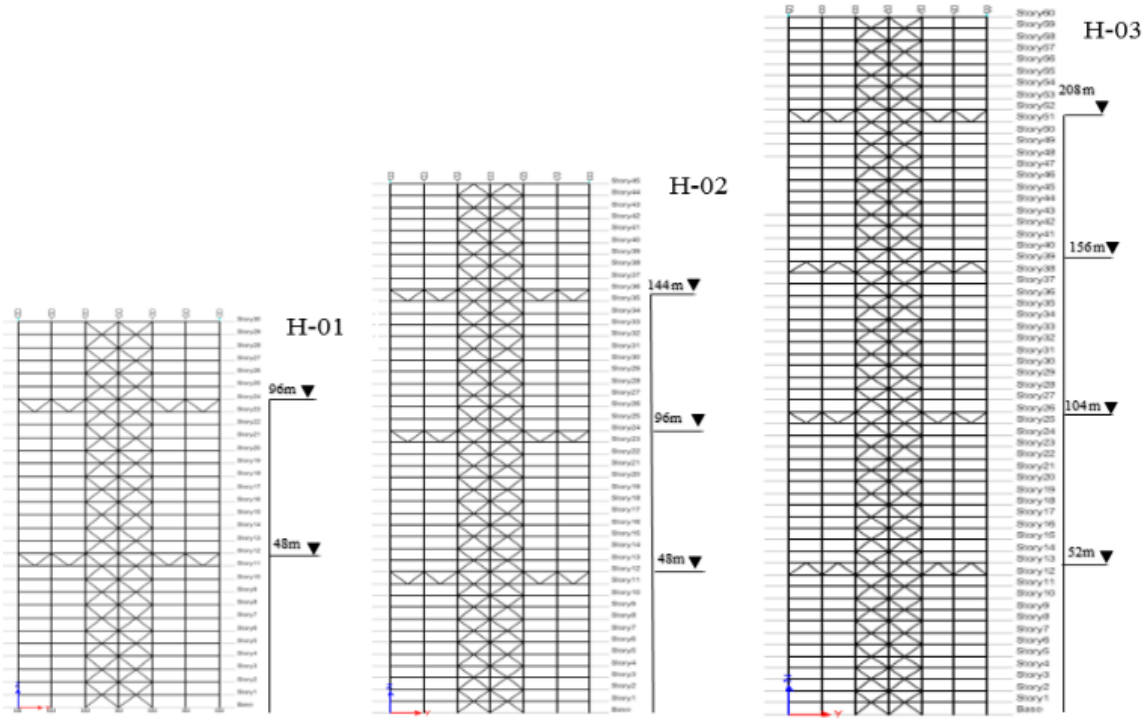

Fig. 1: The overview of the structures of models 30, 45, 60 floors (respectively H-01, H-02, H-03 models)

Table 1: Overall geometry and design loads applied for the studied buildings

	General geometry				Design loads (kg/m^2)					
					FLOOR			ROOF		
	H(M)	FLOOR	S(M)	BAYS	DEAD	LIVE	SNOW	DEAD	LIVE	SNOW
H-01	4	30	8	6×6	453	350	-	412	150	105
H-02	4	45	8	6×6	453	350	-	412	150	105
H-03	4	60	8	6×6	453	350	-	412	150	105

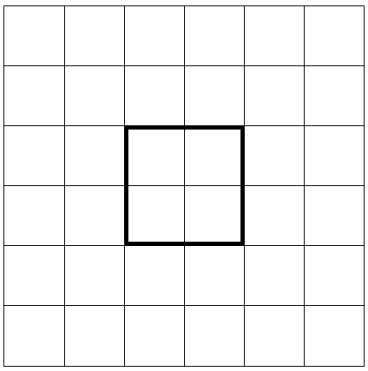

(a) Braced core plan

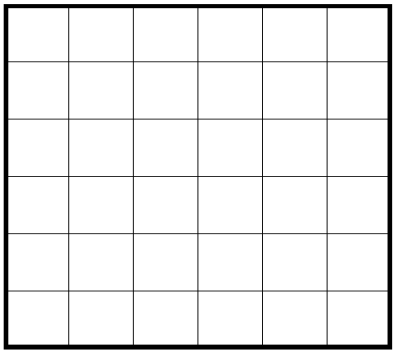

(b) Belt truss plan

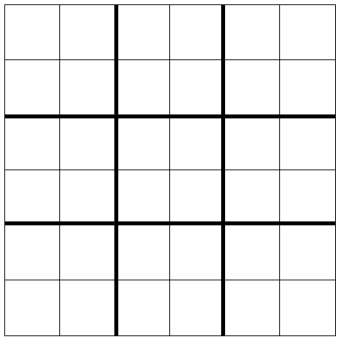

(c) Outrigger arms plan

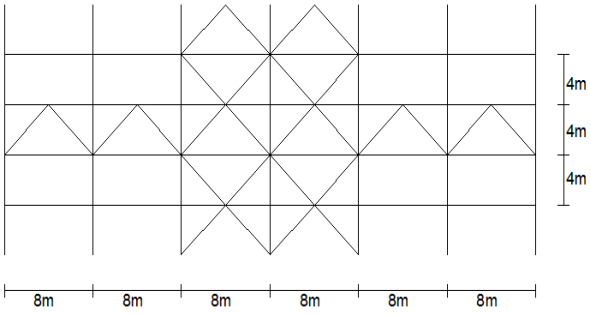

(d)

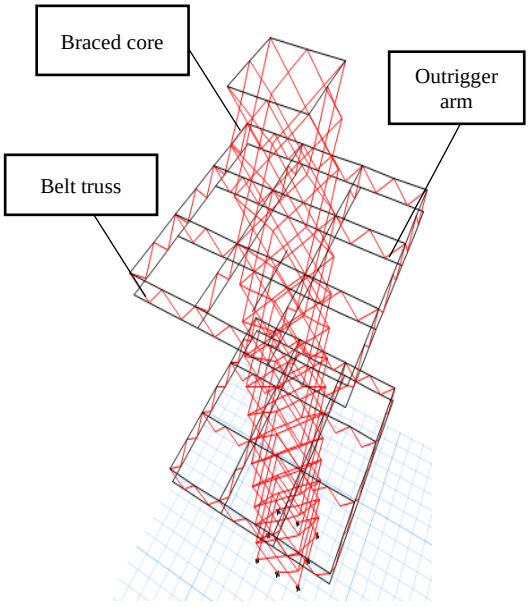

(e)

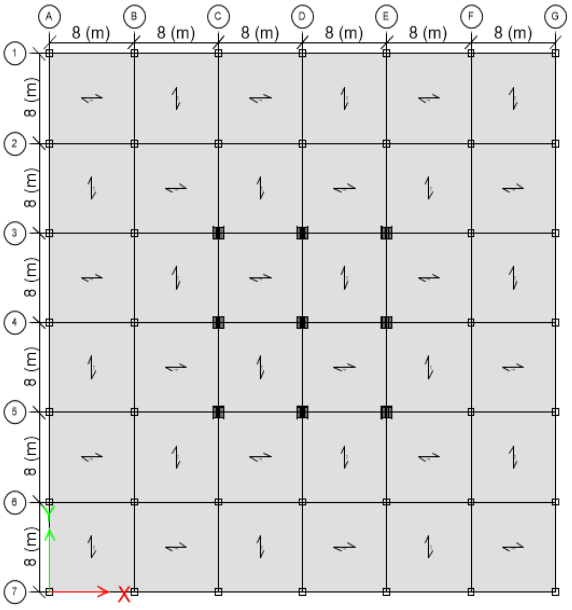

(f)

Fig. 2: (a) Braced core plan (b) Belt truss plan, (c) Outrigger arms plan (d) part of the braced central core and outrigger arm, and (e) how the spans are divided and how the outrigger arms and belt trusses are placed in 3D model,(f) main building plan.

Table 2: H-01 model members sections

Floors	Peripheral column sections	Floors	Middle column sections	Floors	Brace sections	Outrigger arm	Belt truss	Beam
1-5	Box600×40	1-8	Composit1100	1-5	Box320×40	Box400×40	Box200×35	IPE500
6-10	Box550×40	24-9	Box1100×40	6-10	Box300×40			
11-15	Box500×40	25-26	Box850×40	11-15	Box280×40			
16-21	Box450×40	27-28	Box700×40	16-21	Box260×40			
22-25	Box360×40	29-30	Box600×40	22-25	Box240×40			
26-30	Box200×35			26-30	Box220×40			

Table 3: H-02 model members sections

Floors	Peripheral column sections	Floors	Middle column sections	Floors	Brace sections	Outrigger arm	Belt truss	Beam
1-5	Box1000×40T	1-4	Box.C1250×40T	1-9	Box500×40	Box500×40	Box240×40	IPE550
6-10	Box1000×40	5-9	Box.C1200×40T	10-20	Box450×40			
11-15	Box950×40	10-14	Box.C1000×40T	21-30	Box400×40			
16-20	Box850×40	15-19	Box.C1000×40T	31-40	Box360×40			
21-25	Box750×40	20-25	Box950×40	41-45	Box300×40			
26-30	Box700×40	26-30	Box900×40					
31-35	Box650×40	31-35	Box800×40					
36-40	Box550×40	36-40	Box700×40					
41-45	Box450×40	41-45	Box600×40					

Table 4: H-03 model members section

Floors	Peripheral column sections	Floors	Middle column sections	Floors	Brace sections	Outrigger arm	Belt truss	Beam
1-8	Box.C1300×40T	1-8	C.M1300×40T	1-20	Box600×40	Box600×40	Box260×40	IPE600
9-15	Box.C1250×40T	9-15	Box.C1250×40T	21-30	Box500×40			
16-22	Box1200×40T	16-22	Box.C1200×40T	31-40	Box450×40			
23-30	Box1100×40T	23-30	Box.C1100×40T	41-50	Box400×40			
31-35	Box1000×40T	31-36	Box1100×40T	51-60	Box300×40			
36-40	Box1000×40	37-42	Box1000×40					
41-45	Box900×40	43-50	Box900×40					
46-50	Box800×40	51-55	Box800×40					
51-53	Box700×40	56-60	Box700×40					
54-55	Box600×40							
56-57	Box500×40							
58-60	Box400×40							

The design of the members was performed by the dynamic spectral analysis method in soil type D using the combined modal CQC method and the SRSS direction. To assimilate spectral analysis, a linear static analysis was used using ASCE 7-10 Code. Design of all models has been conducted by the Iranian Standard 2800 Ver. 4 and with the help of Sap 2000 Ver. 18.1 software (CSI Sap, 2015) [23]. All sections used in models H-01, H-02, and H-03, are shown in Tables 2 to 4.

2.2 Characteristics of the accelerogram used

In order to perform nonlinear analysis of structural time history, accelerations selection, as well as structural parameters and structural plasticity, are important points in the seismic evaluation of the structure [9]. The accelerometers used to determine the effect of ground motion should be as accurate as possible of the actual movement of the ground at the site of the structure construction when an earthquake happens. In order to achieve this goal, at least three accelerometer pairs belonging to the horizontal components of the three earthquakes which have characteristics similar to those of the construction site, should be selected. In this study, 10 real earthquake records from the Pacific Ocean Earthquake Engineering Research Center (PEER) database (Table 5) were used to achieve this goal. To scale the selected earthquakes with respect to the 5% damping, and D type soil spectrum, the ASCE US 7-10 Code methodology was used, the result of which as scale factor (SF) in two directions are given in Table 5. In Table 5, M_W, Dist, t_{tot} and Vs are respectively the torque magnitudes, the distance from the zone fault, the duration of the earthquake continuation, and the average shear wave velocity of the soil of the area to the depth of 30 meters.

Table. 5: Characteristic of accelerogram applied

Record ID	PEER ID	Event	Station	Component	M_W	Dist (km)	t_{tot} (s)	Vs (m/s)	SF	
									X	Y
1	1233	Chi-Chi, Taiwan	CHY082	E	7.62	36	90	194	2.47	3.66
2	1153	Kocaeli	KOERI Botas	090	7.51	127	102	275	3.25	3.82
3	851	Landers	CDMG 14368 Downey – Co	000	7.28	157	70	272	3.75	1.42
4	1810	Hector	Mecca – CVWD Yard	090	7.13	92	60	345	4.11	3.95
5	1629	St Elias, Alaska	USGS 2728 Yakutat	279	7.54	80	83	275	1.5	
6	777	Loma Prieta	USGS 1028 Hollister City Hall	090	6.93	28	39	199	1.44	2.56
7	1043	Northridge-01	Neenach – Sacatara Ck	090	6.69	52	48	309	4.44	4.59
8	428	Superstition Hills-02	Westmorland Fire Sta	180	6.54	13	40	194	3.98	4.20
9	172	Imperial Valley-06	El Centro Array #1	140	6.53	22	39	237	1.50	2.10
10	2615	Chi-Chi, Taiwan-03	TCU061	N	6.20	40	107	273	2.50	3.82

3. Optimal location of outrigger arms and belt truss

In order to determine the optimum location outrigger arms and belt truss in these three models, these locations are determined based on three methods of energy, Smith's proposed method, and the proposed method of this paper, and the maximum absolute displacement of building roofs and the maximum relative displacement of the floors which are calculated in the dynamic analyses in these models and compared with each other.

3.1 Energy method

The hypotheses governing modeling, using the method presented by Connor and Pouangare [13 and 24], are as follows:

• The behavior of the structure is linear elastic.
• The geometric properties of the core, columns, and outrigger arms are uniform along the height.
• The outrigger arms are rigidly connected to the core and with joints to the outer columns.
• The outrigger arms are considered rigid.
• The effects of the outrigger arms and belt truss are considered in the level connected to the core as screw springs.

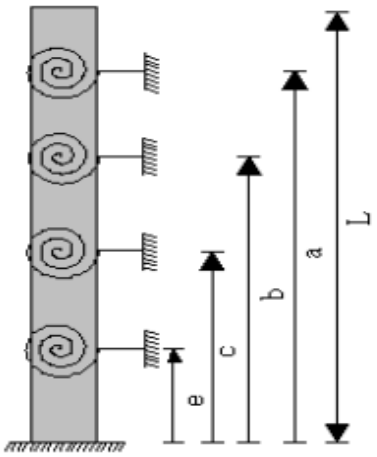

Fig. 3: An analytical model with four outrigger arms at levels (a, b, c and e) [25].

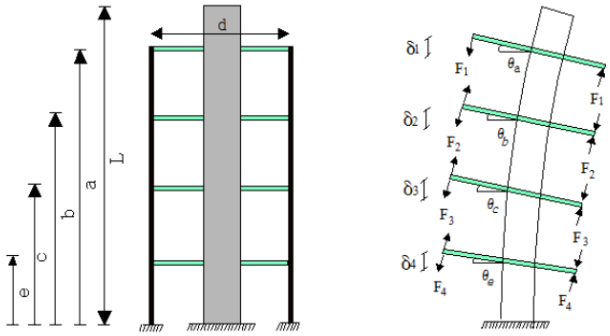

Fig. 4: Equivalent moment of torsional springs with coupling forces [25]

Figure 3 shows an analytical model with four outrigger arms at levels (a, b, c and e). In Figures 3, screw springs are replaced by outrigger arms. In this method, there are spread triangular, trapezoidal, rectangular, and concentrated loading. In this paper, two types of triangular and trapezoidal loadings have been used. To determine the position of the outrigger arms and the belt truss, you need to find a location where the energy absorbed by the screw springs in that location is maximal. As shown in Figure 4, if M is the moment due to a coupling of forces applied to the outrigger arms, the moments M_a, M_b, M_c, and Me can be calculated with the help of Equations (1) to (4). To calculate the rotation amount, equations (5) to (12) can be used. These equations are written for triangular and trapezoid loadings (Figures 5 and 6). The optimum position of the outrigger arms and belt truss are shown in Table (6) with respect to the triangular and trapezoidal loadings. In equations 1 to 13, A means total area and I means moment of inertia.

$$Ma = F1d \quad (1)$$

$$Mb = (F2 - F1)\,d \quad (2)$$

$$Mc = (F3 - F2)\,d \quad (3)$$

$$Me = (F4 - F3)\,d \quad (4)$$

$$\theta a = \frac{\frac{(2ql + ml^2)a^2}{8} - \frac{(3ql^2 + 2ml^3)a}{6} - \frac{qa^3}{6} - \frac{ma^4}{24}}{E.I + E.A.d^2/2} \quad (5)$$

$$\theta b = \frac{\frac{(2ql + ml^2)b^2}{8} - \frac{(3ql^2 + 2ml^3)b}{6} - \frac{qb^3}{6} - \frac{mb^4}{24}}{E.I + E.A.d^2/2} \quad (6)$$

$$\theta c = \frac{\frac{(2ql + ml^2)c^2}{8} - \frac{(3ql^2 + 2ml^3)c}{6} - \frac{qc^3}{6} - \frac{mc^4}{24}}{E.I + E.A.d^2/2} \quad (7)$$

$$\theta e = \frac{\frac{(2ql + ml^2)e^2}{8} - \frac{(3ql^2 + 2ml^3)e}{6} - \frac{qe^3}{6} - \frac{me^4}{24}}{E.I + E.A.d^2/2} \quad (8)$$

$$\theta a = \frac{\frac{hl^2a^2}{4} - \frac{hl^3a}{3} - \frac{ha^4}{24}}{E.I + E.A.d^2/2} \quad (9)$$

$$\theta b = \frac{\frac{hl^2b^2}{4} - \frac{hl^3b}{3} - \frac{hb^4}{24}}{E.I + E.A.d^2/2} \quad (10)$$

$$\theta c = \frac{\frac{hl^2c}{4} - \frac{hl^3c}{3} - \frac{hc^4}{24}}{E.I + E.A.d^2/2}) \quad (11)$$

$$\theta e = \frac{\frac{hl^2e^2}{4} - \frac{hl^3e}{3} - \frac{he^4}{24}}{E.I + E.A.d^2/2} \quad (12)$$

Finally, θ_a and M_a are embedded in Equation (13), and is derived in terms of a, b, c, e.

$$E = \frac{1}{2}M_a\theta_a + \frac{1}{2}M_b\theta_b + \frac{1}{2}M_c\theta_c + \frac{1}{2}M_e\theta_e \quad (13)$$

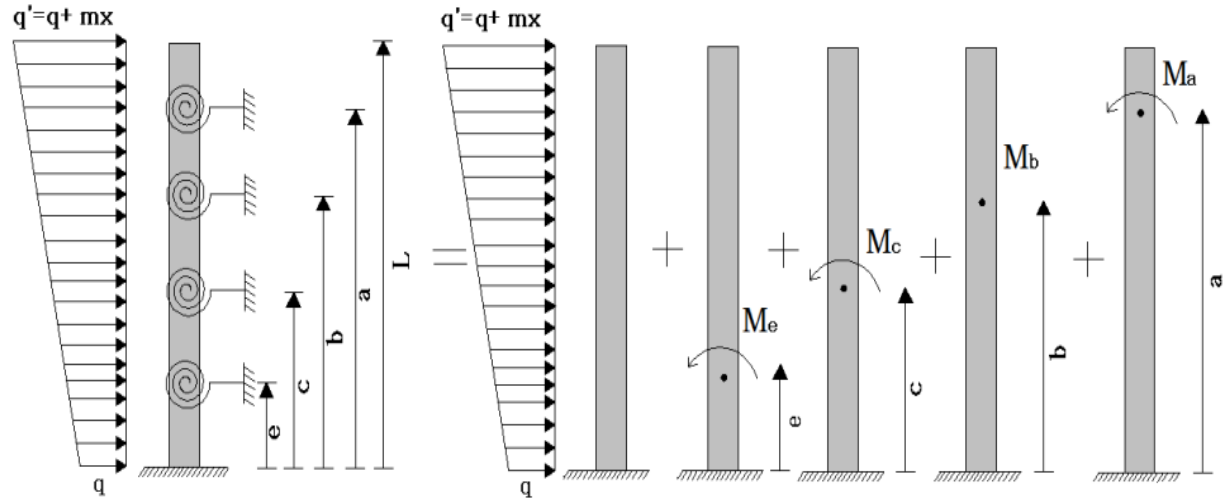

Fig. 5: The analytical model of the high-rise building with four outrigger arms and belt truss under an extensive trapezoidal load [26]

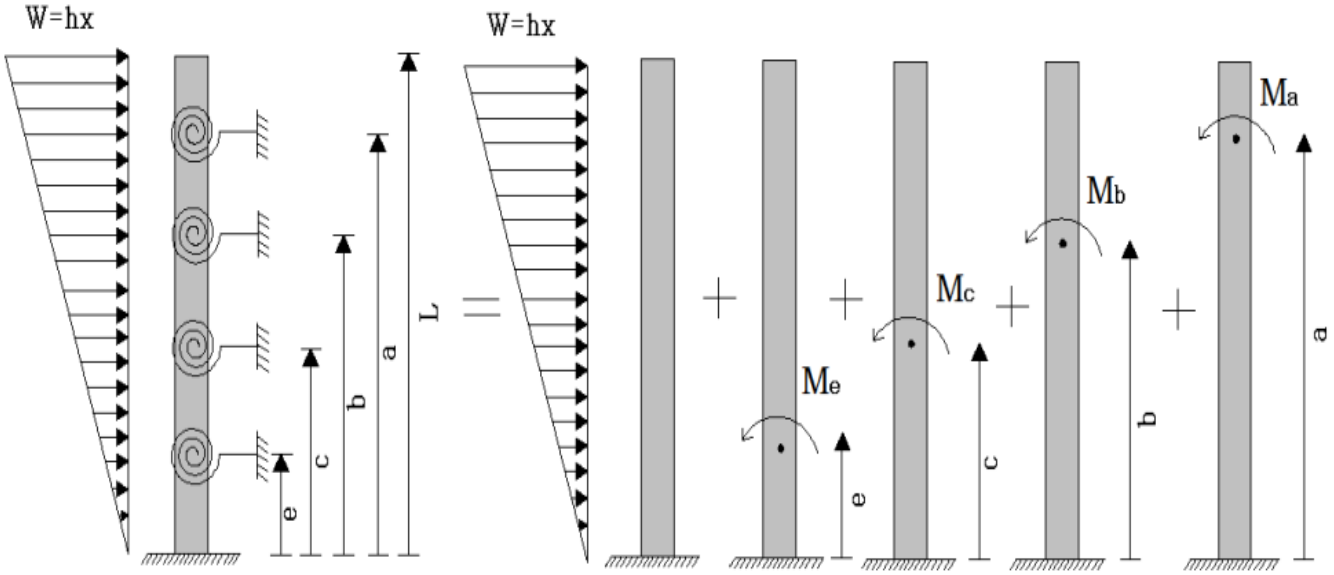

Fig. 6: The analytical model of the high-rise building with four outrigger arms and belt truss under an extensive triangular load [26]

Table. 6: Optimal location of outrigger arms and belt truss under extensive triangular and trapezoidal loads in terms of building height in the energy method

Number of outrigger arms	Position of outrigger arms							
	trapezoidal loading (MPa)				triangular loading (MPa)			
2	0.286	0.620			0.280	0.620		
3	0.203	0.420	0.690		0.208	0.429	0.695	
4	0.158	0.325	0.508	0.734	0.162	0.330	0.510	0.738

According to Table (6), a number of two outrigger arms have been considered for the 30-storey model, three outrigger arms for the 45-storey model, and four outrigger arms for the 60-storey model. The numbers in Table (6) are very close to each other for a building with a number of distinct floors. Therefore, the optimal position of the outrigger arms and belt truss of these two extensive loads are considered the same, and the position with the best results was considered in this paper. The location of the outrigger arms and belt truss is mentioned according to the floors in Table (7).

Table. 7: Location of the outrigger arm based on Energy Method

Number of floors			Location of the outrigger arm
30	18	8	31
45	19	9	31
60	20	10	44

3.2 Smith Method

In Smith's method, in order to minimize the displacement of building floors, and assuming bending rigidity of the outrigger arms, for the optimal performance of the structure with n outrigger arms, the outrigger arms should be at heights of 1/(n + 1) and 2/(n + 1)) to n/(n + 1). The location of the outrigger arms for the models studied based on Smith's method are shown in Table (8).

Table 8: Location of the outrigger arm based on Smith Method

Number of floors			Location of the outrigger arm
30	20	10	34
45	22	11	36
60	24	12	48

3.3 Proposed Method

Based on the dynamic analysis carried out with the help of 10 actual acceleration and spectral analysis, it was observed that for each selected accelerometer, the that the changes of the drift diagram starts from $\frac{1}{3}$ of the height of the structure and ends up to almost $\frac{1}{5}$ of the height of the structure. In the proposed method in this study, the behavior of high-rise building in the height is considered as the behavior of the fixed beam with the same number of outrigger arms, which are along each other along the height of the building, and a fixed beam with an effective length equal to half the effective length of the restrained beams that is placed at the end of the building. For this reason, Equation (14) is proposed to obtain the optimal distance between outrigger arms.

$$\text{Optimal distance of outrigger arms} = \frac{\text{Number of floors}}{\text{number of outrigger arms} + 0.5} \quad (14)$$

The location of outrigger arms based on the proposed method is given in Table (9).optimum location of the outrigger arm and belt truss is not the location determined based on the energy method or the Smith method but a slight change in the location of outrigger arm and belt truss determined according to Smith's method shows that the roof displacement is reduced and the relative displacement of the floors decreases. The behavior of high-rise building by outrigger arm in the proposed method has been shown in the Figure 7.

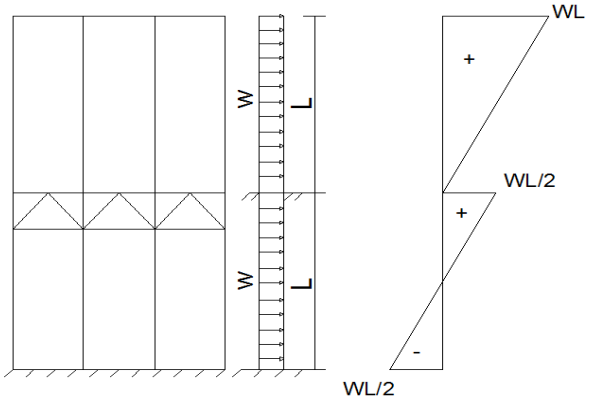

Fig. 7: The behavior of high-rise building by outrigger arm in the proposed method

Table 9: Location of the outrigger arm based on proposed Method

Number of floors	Location of the outrigger arm (in terms of floor)				
30	12	24			
45	13	24		36	
60	13	26	39		52

4. Results and discussion

Three models of 30, 45, and 60 floors using energy,

smith, and proposed methods, which are equipped with outrigger arms and presented in Figure 8, are exposed to the time history analysis and spectral dynamical analysis, and the maximum drifts and maximum absolute displacement of the roofs are shown in Figure 9 and Table 10.

According to the results of Table 10, the proposed method, despite having a very simple equation in comparison to the other two methods, has reduced the maximum displacement of roofs and floors.

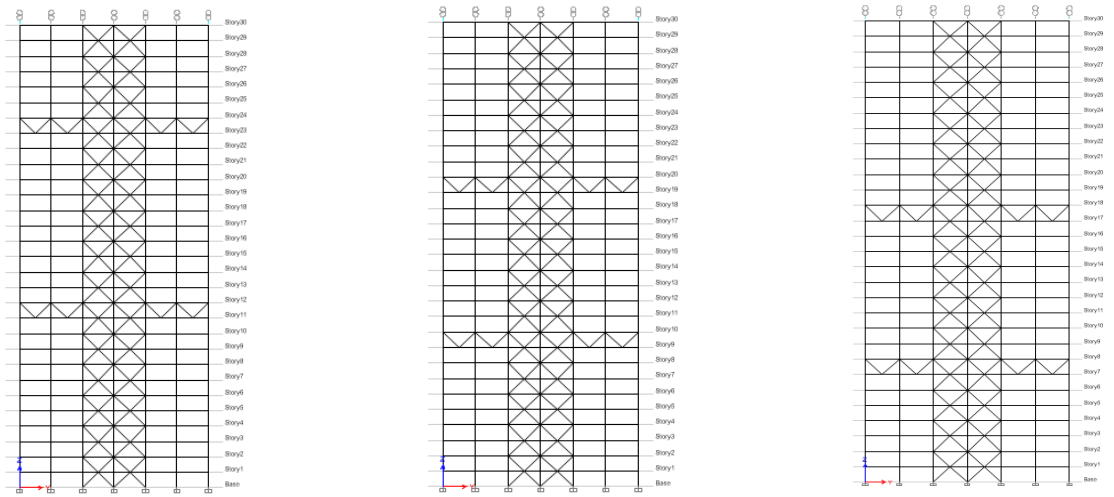

(a) (b) (c)

Fig. 8: Location of the outrigger arms in the 30-storey structure determined by (a) the energy method (b) the Smith method (c) the proposed method

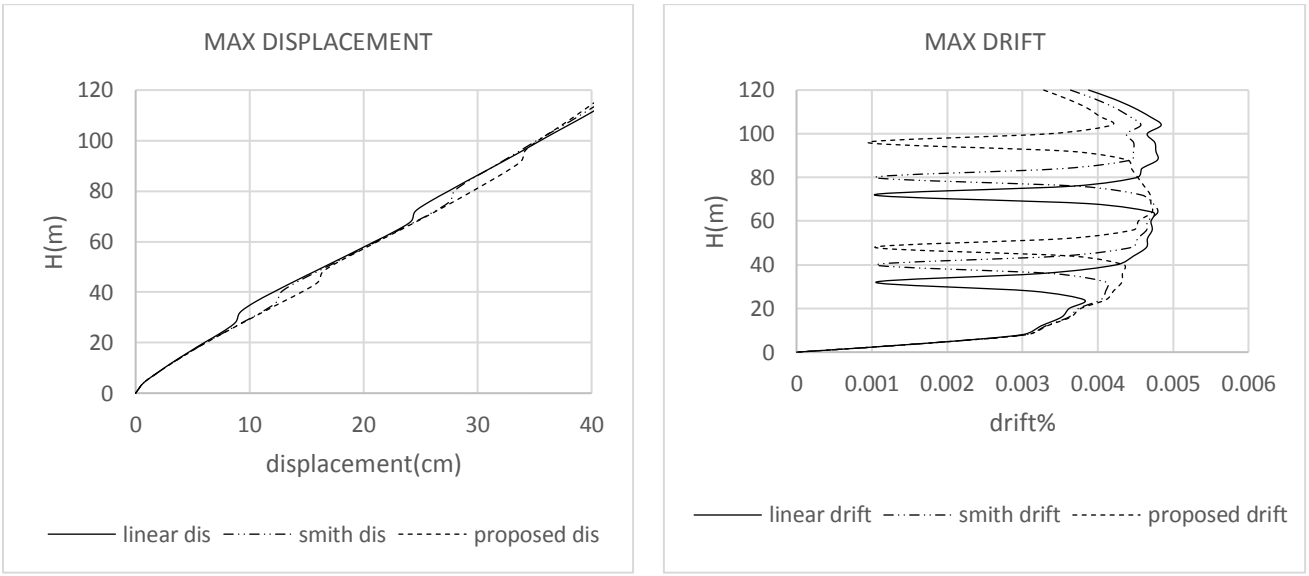

(a) (b)

Fig. 9: Comparison of (a) Maximum roof displacement and (b) Maximum relative displacement of the floors of the 30-storey mode

Table 10: Maximum displacement of roof and maximum relative displacement of floors in a building of 30 floors

Method of determining the optimal location of outrigger arms	Maximum absolute displacement of roof (cm)	Maximum relative displacement of floors (%)
Energy method (linear)	43.22	0.0048715
Smith's method	42.44	0.0048541
Proposed method	41.72	0.0047187

Figure 10 shows the location of outrigger arms and belt truss in the energy of Smith's method, and proposed methods of a 45-storey model, and the graphing comparison and numerical comparison of these three methods are shown in Figure 11 and Table (11), respectively. Regarding the results of nonlinear analysis, the maximum difference in roof displacement of the proposed method is 2 cm in comparison with Smith's method and 5 cm relative to the energy method, whereas, the drift difference of the proposed method is %2.5 compared to Smith's method and %5 relative to the energy method.

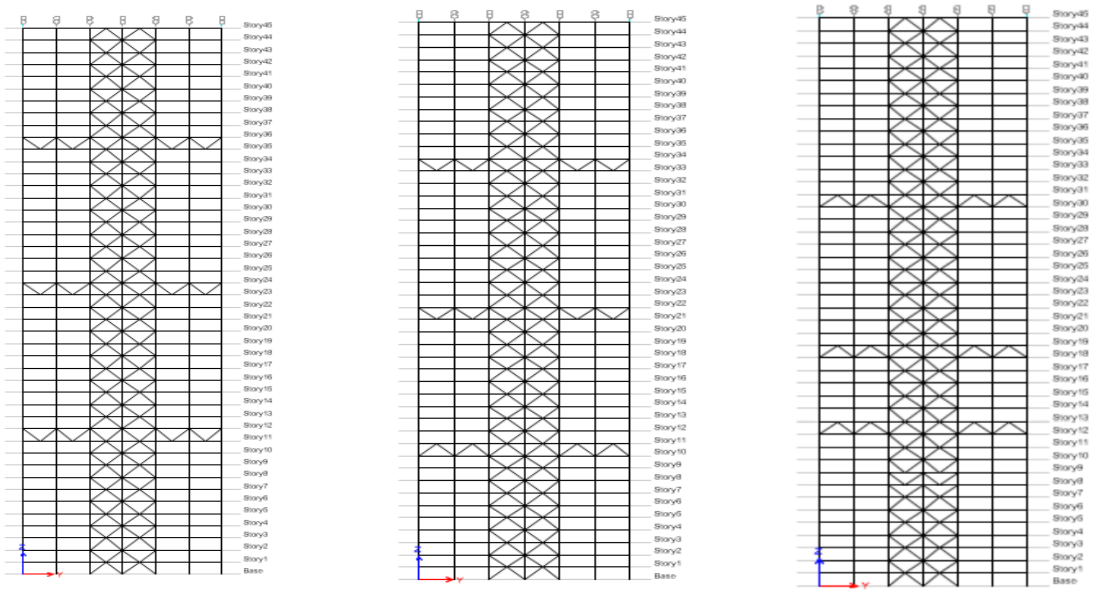

(a) (b) (c)

Fig.10: Location of the outrigger arms in the 45-storey structure determined by (a) the energy method (b) the Smith method (c) the proposed method

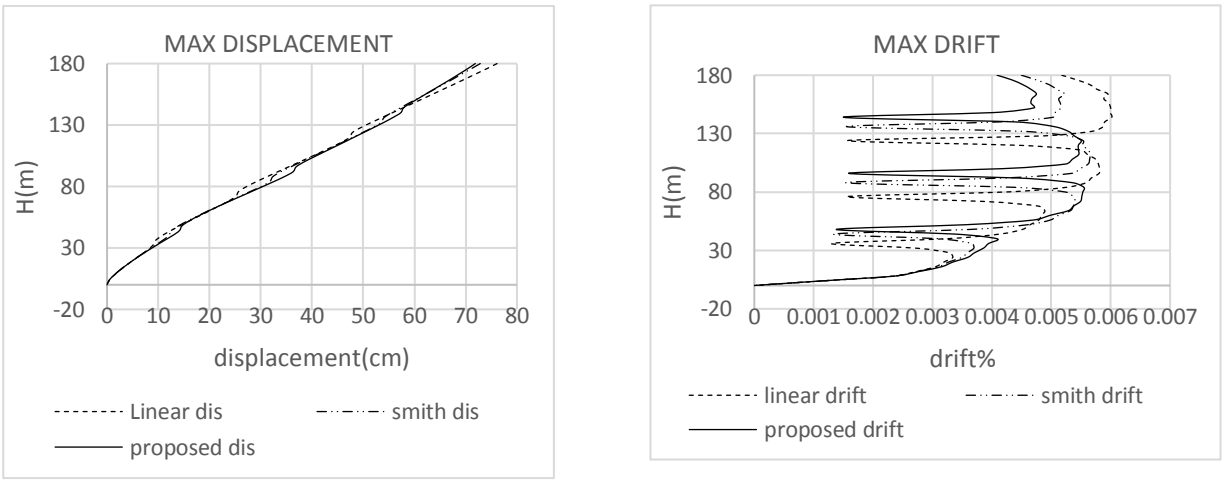

SS(a) (b)

Fig. 11: Comparison of (a) Maximum roof displacement and (b) Max imum relative displacement of the floors of the 45-storey model.

Figure 12 shows the location of outrigger arms and belt truss in the energy, Smith's method, and proposed methods of a 60-storey model, and the graphing comparison and numerical comparison of these three methods are shown in Figure 13 and Table (12), respectively. Regarding the results of nonlinear analysis, the maximum difference in roof displacement of the proposed method is 2 cm in comparison with the Smith method and 2.5 cm relative to the energy method, whereas, the drift difference of the proposed method is %3 compared to Smith's method and %8 relative to the energy method.

Table 11: Maximum displacement of roof and maximum relative displacement of floors in a building of 45 floors

Method of determining the optimal location of outrigger arms	Maximum absolute displacement of roof (cm)	Maximum relative displacement of floors (%)
Energy method (linear)	76.11	0.0060186
Smith's method	73.83	0.0056532
Proposed method	71.87	0.0055491

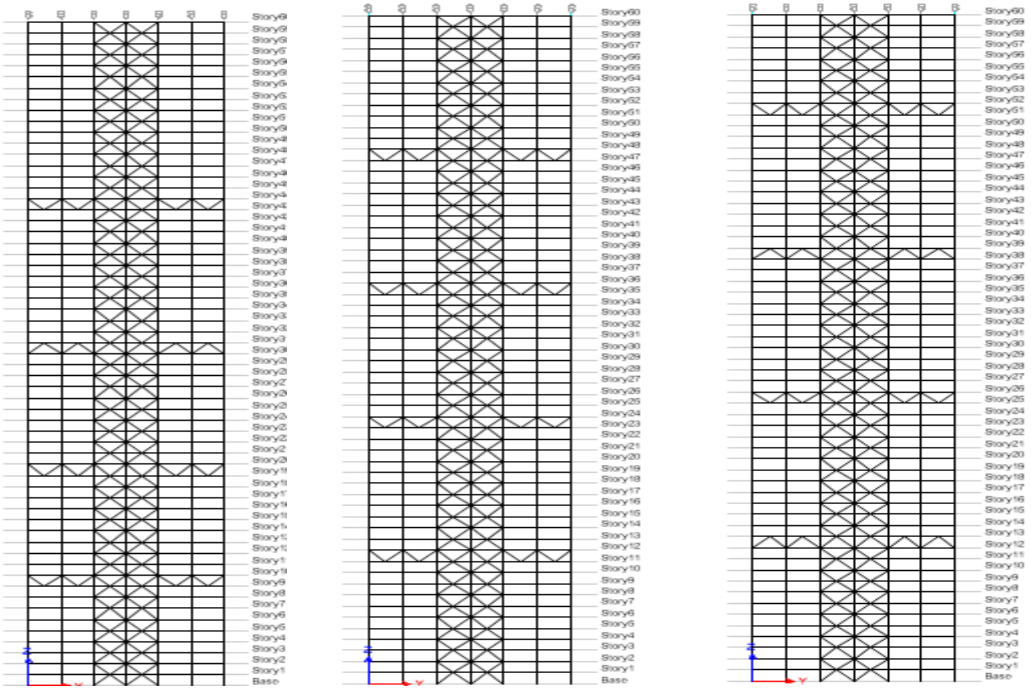

(a) (b) (c)

Fig. 12: Location of the outrigger arms in the 60-storey structure determined by (a) the energy method (b) the Smith method (c) the proposed method.

Table 12: Maximum displacement of roof and maximum relative displacement of floors in a building of 60 floors

Method of determining the optimal location of outrigger arms	Maximum absolute displacement of roof (cm)	Maximum relative displacement of floors (%)
Energy method (linear)	98.25	0.0063841
Smith's method	97.56	0.0062318
Proposed method	95.57	0.0061161

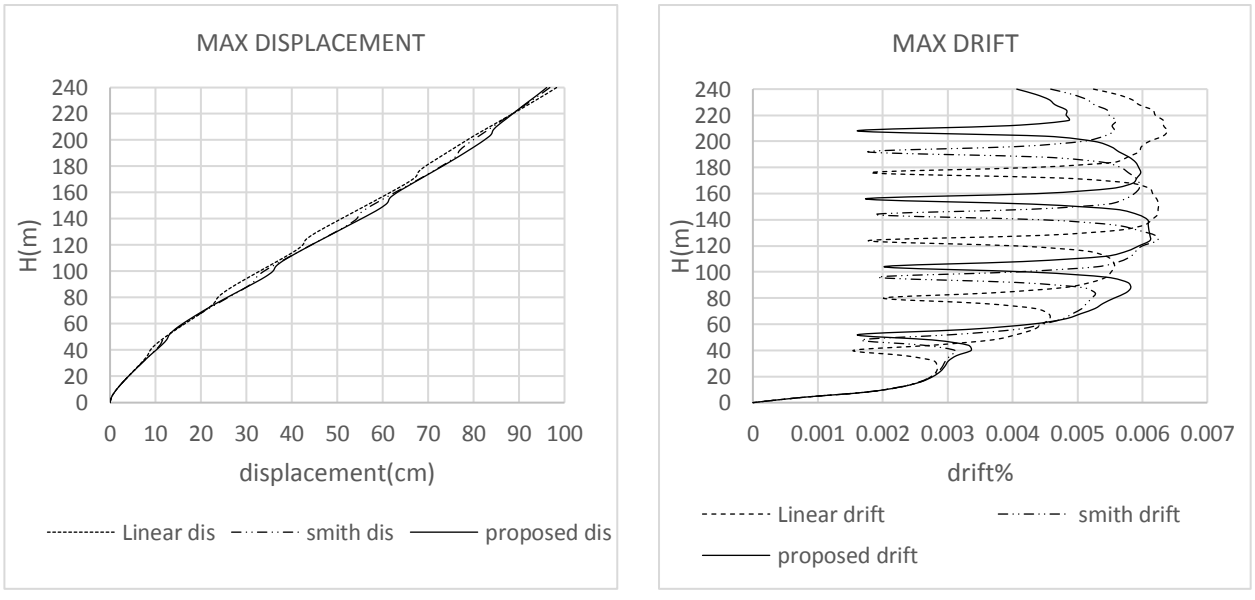

(a) (b)

Fig. 13. Comparison of (a) Maximum roof displacement and (b) Maximum relative displacement of the floors of the 60-storey model

5. Change in the shape of the outrigger arms

One of the problems of the outrigger arm and belt truss structure system with the central core is that, stiffness greatly increases on the floor where the outrigger arm and belt truss is located, and the stress concentration in that floor is very high. Regarding this, in order to control the stress and properly split the force between the members of the structure, the shape of the outrigger arm needs to be corrected so that the stiffness between the upper and lower floors of the outrigger arm is divided and the concentration of stress in some floors is reduced. Assuming that there is a wall on the axes where the outrigger arm is located (A, C, 3.5) and the structure plan can be divided into ten sections, as in Figure 2-c, to reduce the drift and displacement of the roof and reduce the stress concentration in the floor where the outrigger arm exists, the outrigger arm deformation was supplemented by the addition of a diameter bracing, and the results were compared with the original model of the 30-storey building, the outrigger arm location of which was determined by the proposed method.

According to Figure 14-b, in the first step, the middle part was filled with crosswise braces. In this case, it was observed that the stress ratio in some of the braces is very low and these members act as zero-force members and do not have a significant impact on the structure load-bearing. For this reason, this type of braces has been removed and the structure has been deformed to the Figure 14-c. The new model is under dynamic analysis and its results are compared with the model (8-c). As shown in Figure 15, the brace deformation, in addition to having a great influence on the control of the drift and movement of the roof, also greatly reduces the stress concentration in the floors where the outrigger arms are placed, and the graph reaches the floor where the main outrigger arm exists, with a mild slope. The reason for this is that, in the new bracing model, the structure stiffness has not suddenly changed, and its stress concentration on the columns of that floor has been greatly reduced, the results of which are given numerically in Table (13). According to the results of Table (13), it is observed that the difference in the displacement of the roof with the deformation of the outrigger arm, has been significantly reduced, and the roof displacement difference has been recorded 7.08 cm (21%), and the drift difference is 18%. ‘

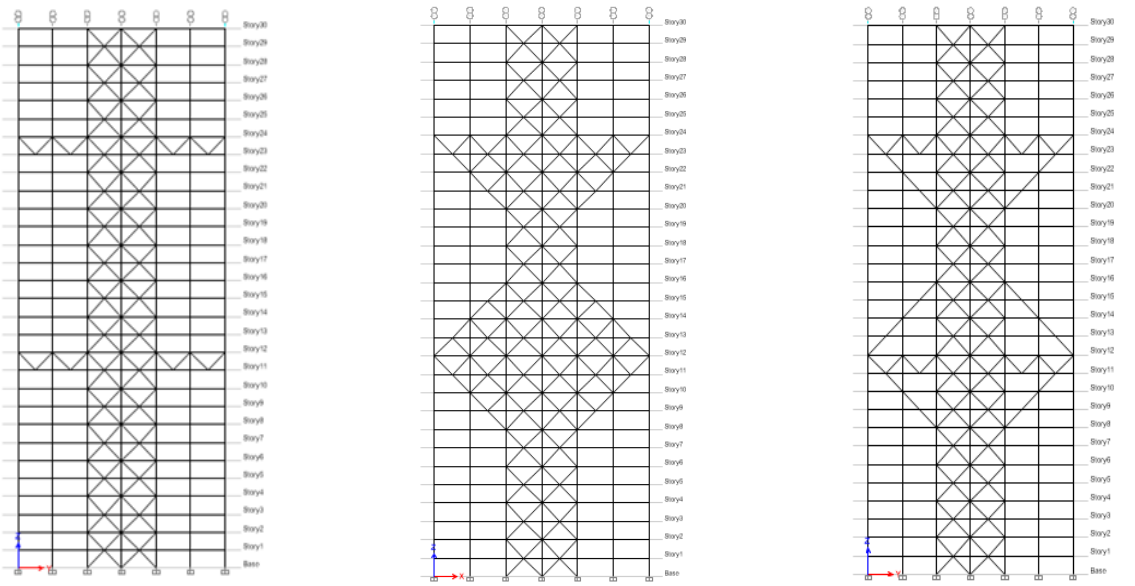

(a) (b) (c)

Fig. 14: (a) Optimal location of the outrigger arms based on the proposed method (b) The initial deformation of the outrigger arms (c) final modified form of the outrigger arms

Table 13: Maximum displacement of roof and maximum relative displacement of floors in a building of 60 floors

Shape of outrigger arms	Maximum absolute displacement of roof (cm)	Maximum relative displacement of floors (%)
Energy method (linear)Initial form	41.72	0.0047187
Final modified form	34.64	0.0040833

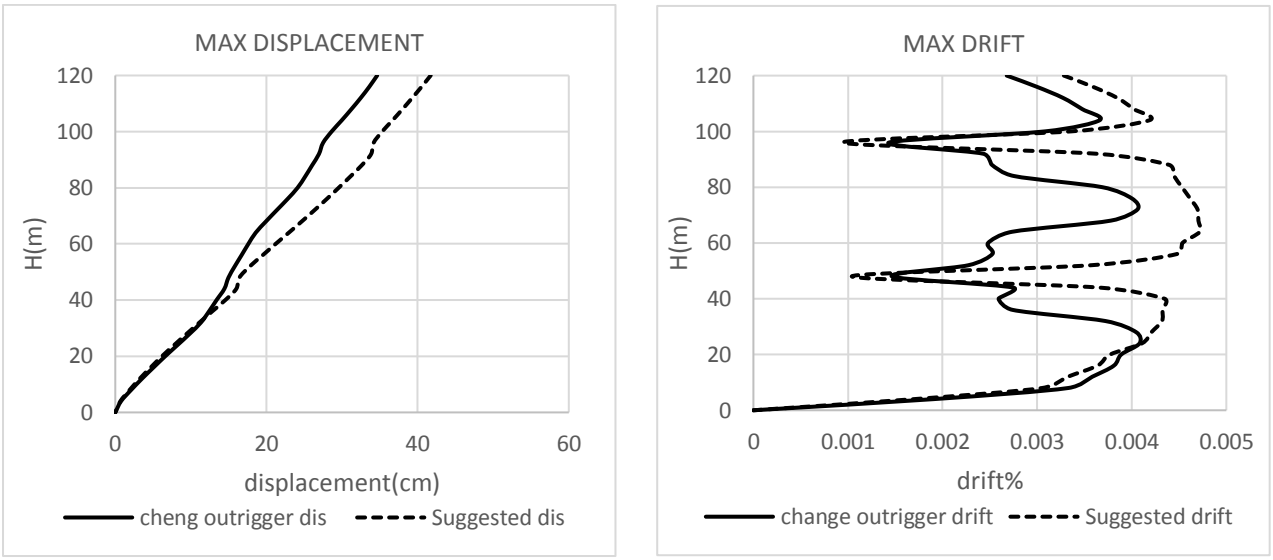

(a) (b)

Fig. 15: Comparison of (a) Maximum displacement of the roof and (b) Maximum relative displacement of the floors of the 30-story building with the initial and final modified shapes of outrigger arms

Table 13: Maximum displacement of roof and maximum relative displacement of floors in a building of 60 floors

Shape of outrigger arms	Maximum absolute displacement of roof (cm)	Maximum relative displacement of floors (%)
Energy method (linear)Initial form	41.72	0.0047187
Final modified form	34.64	0.0040833

6. Conclusion

In this research, while offering a very simple method for determining the optimum location of outrigger arms and belt truss in high-rise buildings with a central core and comparing the results of this proposal with other available methods, some recommendations were also presented for the modification of the shape of the outrigger arms and the implications of these suggestions in 30, 45 and 60-storey buildings have been evaluated with dynamic analyses. Based on the proposed method, the maximum absolute roof displacement and maximum relative displacement of floors decreased in all models compared to other methods, and by modifying the shape of the outrigger arms and avoiding a sudden change in the lateral stiffness at the height of the building, the concentration of force is reduced in the floors where outrigger arms are installed, and the stresses are distributed more uniformly at the building's height.

References

[1] Smith, B. S., Coull, A., & Stafford-Smith, B. S. (1991). *Tall building structures: analysis and design* (Vol. 5). New York: Wiley.

[2] Meftah, S. A., Tounsi, A., & El Abbas, A. B. (2007). A simplified approach for seismic calculation of a tall building braced by shear walls and thin-walled open section structures. *Engineering Structures*, *29*(10), 2576-2585.

[3] Ji, J., Elnashai, A. S., & Kuchma, D. A. (2007). An analytical framework for seismic fragility analysis of RC high-rise buildings. *Engineering structures*, *29*(12), 3197-3209.

[4] Khoshnoudian, F., & Kashani, M. M. B. (2012). Assessment of modified consecutive modal pushover analysis for estimating the seismic demands of tall buildings with dual system considering steel concentrically braced frames. *Journal of Constructional Steel Research*, *72*, 155-167.

[5] Kheyroddin, A., & Aramesh, S. (2015). Lateral Resisting System inTall Buildings.

[6] Montuori, G. M., Mele, E., Brandonisio, G., & De Luca, A. (2014). Design criteria for diagrid tall buildings: Stiffness versus strength. *The Structural Design of Tall and Special Buildings*, *23*(17), 1294-1314.

[7] Montuori, G. M., Mele, E., Brandonisio, G., & De Luca, A. (2014). Geometrical patterns for diagrid buildings: Exploring alternative design strategies from the structural point of view. *Engineering Structures*, *71*, 112-127.

[8] Montuori, G. M., Mele, E., Brandonisio, G., & De Luca, A. (2014). Secondary bracing systems for diagrid structures in tall buildings. *Engineering Structures*, *75*, 477-488.

[9] Takewaki, I., Murakami, S., Fujita, K., Yoshitomi, S., & Tsuji, M. (2011). The 2011 off the Pacific coast of Tohoku earthquake and response of high-rise buildings under long-period ground motions. *Soil Dynamics and Earthquake Engineering*, *31*(11), 1511-1528.

[10] Trabelsi, A., Kammoun, Z., & Beddey, A. (2017). Seismic retrofitting of a tower with shear wall in UHPC based dune sand. *Earthquakes and Structures*, *12*(6), 591-601.

[11] Coull, A., & Bose, B. (1975). Simplified analysis of frame-tube structures. *Journal of the Structural Division*, *101*(11), 2223-2240.

[12] Coull, A., & Ahmed, A. K. (1978). Deflections of framed-tube structures. *Journal of the Structural Division*, *104*(5), 857-862.

[13] Connor, J. J., & Pouangare, C. C. (1991). Simple model for design of framed-tube structures. *Journal of structural engineering*, *117*(12), 3623-3644.

[14] Moghadam, M. A., Meshkat-Dini, A., & Moghadam, A. S. (2015, May). Seismic performance of steel tall buildings with outrigger system in near fault zones. In *Proceedings of the 7th International Conference on Seismology & Earthquake Engineering*.

[15] Brunesi, E., Nascimbene, R., & Casagrande, L. (2016). Seismic analysis of high-rise mega-braced frame-core buildings. *Engineering Structures*, *115*, 1-17.

[16] Kim, J., & Park, J. (2012). Progressive collapse resisting capacity of building structures with outrigger trusses. *The Structural Design of Tall and Special Buildings*, *21*(8), 566-577.

[17] Chen, Y., & Zhang, Z. (2018). Analysis of outrigger numbers and locations in outrigger braced structures using a multiobjective genetic algorithm. *The Structural Design of Tall and Special Buildings*, *27*(1), e1408.

[18] Hoenderkamp, J. C. D. (2008). Second outrigger at optimum location on high-rise shear wall. *The structural design of tall and special buildings*, *17*(3), 619-634.

[19] Kim, H. S., & Kang, J. W. (2017). Smart outrigger damper system for response reduction of tall buildings subjected to wind and seismic excitations. *International journal of steel structures*, *17*(4), 1263-1272.

[20] Kamgar, R., & Rahgozar, R. (2017). Determination of optimum location for flexible outrigger systems in tall buildings with constant cross section consisting of framed tube, shear core, belt truss and outrigger system using energy method. *International Journal of Steel Structures*, *17*(1), 1-8.

[21] Standard 2800 (2019), Iranian code of practice for seismic resistant design of buildings standard No. 2800, Version 4

[22] Kim, S., & D'Amore, E. (1999). Push-over analysis procedure in earthquake engineering. *Earthquake Spectra*, *15*(3), 417-434.

[23] Sap 2000 (2015). Structural analysis program (SAP). Computers and Structures, Inc, Version 18.01, USA.

[24] Faghihmaleki, H., & Abdollahzadeh, G. (2019). Using risk-based robustness index for seismic improvement of structures. *KSCE Journal of Civil Engineering*, *23*(3), 1207-1218.

[25] Taranath, B. S. (1975). Optimum belt truss location for high-rise structures. *Structural Engineer* 53(8), 18-21.

[26] Jahanshahi, M. R., & Rahgozar, R. (2013). Optimum location of outrigger-belt truss in tall buildings based on maximization of the belt truss strain energy.